Atmos. Meas. Tech. Discuss., 7, 6359–6384, 2014
www.atmos-meas-tech-discuss.net/7/6359/2014/
doi:10.5194/amtd-7-6359-2014

Atmospheric Measurement Techniques Discussions

Dual channel photoacoustic hygrometer for airborne measurements: background, calibration, laboratory and in-flight inter-comparison tests

D. Tátrai[1,2], Z. Bozóki[1,2], H. Smit[3], C. Rolf[4], N. Spelten[4], M. Krämer[4], A. Filges[5], C. Gerbig[5], G. Gulyás[6], and G. Szabó[1,2]

[1]University of Szeged, Department of Optics and Quantum Electronics, Szeged, Hungary
[2]SZTE-MTA Research Group on Photoacoustic Spectroscopy, Hungary
[3]Forschungszentrum Jülich, Institute for Energy and Climate Research Troposphere (IEK-8), Jülich, Germany
[4]Forschungszentrum Jülich, Institute for Energy and Climate Research Stratosphere (IEK-7), Jülich, Germany
[5]Max Planck Institute for Biogeochemistry, Department of Biogeochemical Systems, Jena, Germany
[6]Hilase Ltd., Szeged, Hungary

Received: 12 April 2014 – Accepted: 19 May 2014 – Published: 26 June 2014

Correspondence to: D. Tátrai (tatraid@titan.physx.u-szeged.hu)

Published by Copernicus Publications on behalf of the European Geosciences Union.

AMTD
7, 6359–6384, 2014

Abstract

This paper describes a tunable diode laser based dual channel photoacoustic (PA) humidity measuring system called WaSul-Hygro primarily designed for aircraft based environment research. It is calibrated for total pressures and water vapor (WV) volume mixing ratios (VMRs) possible during airborne applications. WV VMR is calculated by using pressure dependent calibration curves and a cubic spline interpolation method. Coverage of the entire atmospheric humidity concentration range which might be encountered during airborne measurements is facilitated by applying an automated sensitivity mode switching algorithm. The calibrated PA system was validated through laboratory and airborne inter-comparisons, which proved that the repeatability, the estimated accuracy and the response time of the system is 0.5 ppmV or 0.5 % of the actual reading (whichever value is the greater), 5 % of the actual reading within the VMR range of 1–12 000 ppmV and 2 s, respectively. The upper detection limit of the system is about 85 000 ppmV, limited only by condensation of water vapor on the walls of the 318 K heated PA cells and inlet lines. The unique advantage of the presented system is its applicability for simultaneous water vapor and total water volume mixing ratio measurements.

1 Introduction

This paper describes a tunable diode laser based dual channel photoacoustic (PA) humidity measuring system primarily designed for aircraft based environment research. It is calibrated for total pressures and water vapor (WV) volume mixing ratios (VMRs) possible during airborne applications. WV VMR is calculated by using pressure dependent calibration curves and a cubic spline interpolation method. Coverage of the entire atmospheric humidity concentration range which might be encountered during airborne measurements is facilitated by applying an automated sensitivity mode switching algorithm. The calibrated PA system was validated through laboratory and airborne

AMTD
7, 6359–6384, 2014

inter-comparisons, which proved that the repeatability, the estimated accuracy and the response time of the system is 0.5 ppmV or 0.5 % of the actual reading (whichever value is the greater), 5 % of the actual reading within the VMR range of 1–12 000 ppmV and 2 s, respectively. The upper detection limit of the system is about 85 000 ppmV, limited only by condensation of water vapor on the walls of the 318 K heated PA cells and inlet lines. The unique advantage of the presented system is its applicability for simultaneous water vapor and total water volume mixing ratio measurements.

2 Experimental

2.1 The photoacoustic system

The PA effect is the conversion of electromagnetic radiation into acoustic waves (Bell, 1880, 1881). Whenever a gas absorbs intensity- or wavelength-modulated light, the absorbed light energy is converted into acoustic waves via non-radiative relaxation processes. These acoustic waves can be considerably amplified by using a properly designed PA cell, through which the analyzed gas sample flows, and by setting the light source modulation frequency to coincide with a selected acoustic resonance frequency of the PA cell. The generated and amplified acoustic wave can be detected by a sensitive microphone. The amplitude of the acoustic signal at the frequency of the modulation of the light source usually determined by using lock-in signal processing technique is proportional to the concentration of the light absorbing molecules (McDonald and Wetsel, 1978). In the following the determined lock-in value is referred as PA signal. This measurement technique has been discussed in details in several publications (Castleden et al., 1981; Schilt and Thevanaz, 2006; Saarela et al., 2009; Bozóki et al., 2011).

The layout of WaSul-Hygro, which is placed into a 19″ 3U height rack and has a weight of about 15 kg, can be seen in Fig. 1. Its custom controlling electronics is based on a Digital Signal Processor (DSP) and programmed for signal generation, data

AMTD
7, 6359–6384, 2014

acquisition and operation control. Its main parts are a diode laser current driver, a programmable gain dual channel microphone amplifier, a synchronized sampling based dual channel digital lock-in detector, temperature stabilization units both for the laser and the detection cells, analogue and digital in- and outputs for sensor signal reading and controlling the supplementary components of the system.

The light source is a room temperature operated, optical fiber coupled, distributed feedback diode laser (NEL NLK1E5E1AA). To stabilize and set the emission wavelength the laser temperature can be accurately adjusted and stabilized with the help of a Peltier-cell and a thermistor both built into the housing of the laser (Seufert et al., 2004) and by applying a PID (proportional-integral-derivative) control algorithm. The tuning range of the laser extends from 1391 to 1394 nm where water vapor has several absorption lines and the measurements were performed on the strongest one i.e. @1392.535 nm, where the maximum optical absorption coefficient of 1 ppmV VMR of water vapor is $3.7 \times 10^{-5}\,\mathrm{m}^{-1}$ at 1 bar pressure (Sharpe et al., 2004). The laser in the system is wavelength modulated: periodically on and off tuned to the peak of the absorption line. Such modulation is optimal for the detection of molecules having narrow absorption lines while it reduces the level of PA signal generated by interfering broad absorption features of e.g. large molecules, atmospheric aerosols or pollutants condensing on the windows of the PA cell.

In order to maximize the sensitivity of the PA system, which is defined as the PA signal change caused by unit change in humidity, the amplitude of the laser modulation has to be optimized for the width of the absorption line (Szakáll et al., 2006), which strongly depends on the total gas pressure (Buldyreva et al., 2011). Taking into account that humidity typically decreases with decreasing air pressure (i.e. with increasing altitude) it is reasonable to optimize the laser modulation at a low pressure (in the current case at 200 hPa) in order to have maximum sensitivity at low concentrations. Furthermore the sensitivity of WaSul-Hygro decreases with decreasing pressure due to the acoustic properties of the PA cell. These two effects make the pressure dependence of the sensitivity rather complicated (Sect. 3.1).

AMTD
7, 6359–6384, 2014

WaSul-Hygro includes two PA cells having the so called longitudinal differential cell construction (Miklós et al., 2001) milled into a stainless steel block with the dimensions 10 cm × 10 cm × 4 cm (length by width by height). The cells are fixed together in a way that they have one common window through which the output excitation laser light from the first cell enters directly into the second cell. The cells are thermally isolated from their surrounding and equipped with a resistive heater and a PT100 thermistor. As sound velocity and consequently the acoustic resonance frequency of the PA cell is proportional to the square root of temperature, in order to avoid uncontrolled variation of the acoustic resonance frequencies the temperature of the cells are stabilized to 318 ± 0.1 K using pulse with modulation algorithm. At this temperature each cell has the acoustic resonance frequency of 4500 Hz.

The microphone signals are amplified electrically by an INA163 instrumentation amplifier; the gain of the amplifier can be programmatically set to be either 60 or 600. The amplified microphone signals from both measuring cells are simultaneously and continuously sampled by the analogue to digital converters (ADC) of the controlling electronics into sequences having duration of about 2 s. This temporal resolution of the measurements was selected because 2 s is also the response time of the combination of the PA cells and the inlet system to sudden humidity variation.

As it can be seen in Fig. 1 the gas handling of the PA system contains temperature stabilized (heated to 318 ± 1 K) inlet lines, pressure sensors (Druck PMP 1400 series, 0–1.5 bar absolute) right after the PA cells, and mass flow controllers (Mykrolis Tylan FC2900, 0–1 slpm (standard liter per minute)) which set the volume flow rates to 0.4 slpm. During airborne operation gas flow through the cells can be maintained either by the ram pressure at the sampling inlet of the aircraft or by a downstream vacuum pump. The former and the latter cases are typically realized by a forward and a sideward (or backward) facing sampling inlet, which can be used for TW and WV sampling, respectively. Elements of the gas handling are connected by 6 mm outer diameter stainless steel tubes and Swagelok connectors.

AMTD
7, 6359–6384, 2014

The measured PA signals, the pressures within the PA cells, and supplementary measurement information (like temperature values and self-checking results) are transferred to a data logging PC connected to the electronics via serial port. Software written in LabVIEW graphical programming language (National Instruments) running on a PC calculates humidity values in real-time from the measured data by using the calibration parameters (Sects. 2.2.4, 2.3 and 3.1).

2.2 Special features of the PA system

Compared to its earlier versions the presented system has several novel features, which were developed in order to improve the reliability of its operation.

2.2.1 Dual channel operation

The dual channel construction of the system can be used either to increase the signal to noise ratio of a single stream measurement by averaging the VMR readings of the two channels, or to measure humidity simultaneously in two different gas streams. In the latter case the system can be used for simultaneous VW and TW (after evaporation in the tubes) VMR measurement whenever a proper inlet system is used like in the CARIBIC project (Brenninkmeijer et al., 2007) or for the validation and comparison of different sampling systems. As most of the setup (controlling electronics, laser) are common for the two cells small differences between the VMR values in the sampling lines are expected to be measurable more accurately with the presented system rather than using separate systems for each sampling line.

2.2.2 Sensitivity mode switching

Proportionality between the PA signal and the measured water vapor concentration holds over at least 5 orders of magnitudes but the measurement range of the controlling electronics in its actual configuration cannot cover the entire range of interest because the amplified microphone signal at high concentrations overloads the input of

AMTD
7, 6359–6384, 2014

the ADC. To increase the measurement range of the electronics a sensitivity mode (SM) switching algorithm is implemented in the DSP software, which automatically switches the microphone gain from 600 to 60 (or from 60 to 600) whenever the PA signal becomes higher (or lower) than a certain limit. Hysteresis between the switching limits is introduced in order to avoid frequent switching generated by small-scale signal fluctuations. The change in the SM makes it possible to extend the upper limit of the measure range to 30 000 ppmV. Above this concentration the AD converter saturates again therefore the PA signal has to be decreased further. This can be achieved by de-tuning the laser modulation frequency from the resonance frequency of the cell. This extends the measurement range with at least an order of magnitude but above about 85 000 ppmV water vapor starts condensating in the PA cell or in the sampling line. However such high WV VMR is really unlikely to occur during airborne measurements. Actually the highest humidity level measured during the tests described in Sects. 2.4 and 2.5 was below 30 000 ppmV so the off-resonant modulation was not applied.

2.2.3 Laser wavelength stabilization

The lower the pressure is, the narrower the water vapor absorption lines are, and consequently the wavelength stability of the laser becomes a more and more critical issue. The wavelength of a properly temperature stabilized laser can vary spontaneously due to the so called ageing effects (Woodward et al., 1993) therefore a wavelength locking method (WLM) (Tátrai et al., 2013; Bozóki et al., 2013) with which the laser wavelength can be measured and set with at least 25 fm accuracy with a one second execution time is applied. This wavelength uncertainty can cause less than 0.1 % error in the measured VMR values at any pressures. As the laser ageing effect becomes significant only on a rather long time scale, it is sufficient to perform the WLM only once during each flight, preferably after the Wasul-Hygro system is switched on and the aircraft is before take-off.

AMTD
7, 6359–6384, 2014

2.2.4 Real-time VMR calculation

The input parameters for the VMR calculation for both two cells are: the PA signals, the pressures in the cells, the actual SMs and the calibration curves (Sects. 2.3 and 3.1) which form the calibration surface in the PA signal–pressure–VMR space. To calculate VMR a two-step approach is used: first VMRs are calculated from the PA signals for all the 10 calibration pressures, and then from the resulting dataset the actual VMR is determined by interpolation to the actual pressure using a cubic spline algorithm. The execution time of this method is in the orders of milliseconds by using a general purpose PC or notebook giving the possibility for real-time VMR calculation.

2.3 Calibration of the PA system

In order to have a simple but reliable tool for the calibration through a wide concentration range and at various pressures a set-up shown in Fig. 2 including a home-made humidity generator (HG) and a reduced pressure stabilizer was assembled around WaSul-Hygro. Its automatic operation is ensured by including a stepper motor controlled needle valve, which together with the MFCs inside WaSul-Hygro and with a downstream pump reduces and stabilizes the pressure within the PA cells with ±1 hPa accuracy. The central part of the HG is a saturator having a spiral with 95 cm length milled into a 12 cm × 12 cm × 6 cm cooper block hermetically sealed from its surrounding. Thanks to an overpressure reduction tube, which is long enough to avoid back diffusion of water vapor from ambient air and installed to eliminate the non-synchronizability of the MFC-s just before the saturator, the HG is operated close to atmospheric pressure.

At the beginning of the calibration liquid nitrogen is poured into the HG, which cools down the saturator to around 120–140 K, and then the saturator slowly (approximately during one and a half day) warms up to room temperature. Inside the saturator there is always ice or liquid water on the walls serving as a source for water vapor during warm-up so the VMR will always correspond to the saturation pressure of water vapor at the temperature of the saturator. By measuring the temperature of the saturator

AMTD
7, 6359–6384, 2014

with a PT100 thermistor and the gas pressure inside with a pressure sensor (Druck PMP 1400 series 0–1.5 bar absolute), the generated WV VMR can be calculated by using the Goff–Gratch equation (Goff and Gratch, 1946; WMO-Report No. 8, 1983). This HG was calibrated against a chilled mirror hygrometer at the Hungarian National Office of Measures in the 1–25 000 ppmV range. During this calibration an offset of 1.2 K was found between the measured temperature of the saturator and the actual dew/frost point. After correcting this offset the repeatability of water vapor generation at any temperature was found to be ±0.5 % of the actual VMR or ±0.3 ppmV (the higher value applies).

The slow warm up of the saturator makes it possible to repeatedly vary the gas pressure between 80, 130, 150, 200, 280, 370, 500, 650, 800 and 970 hPa, and also to repeat the PA measurements with the two different SMs. In this way during a single warm up of the HG 20 different calibrations can be completed for each PA cell.

2.4 Verification of the calibration

The PA system was blind tested at Research Center Jülich (Germany) at the Environmental Simulation Facility (ESF) chamber (Smit et al., 2000). The chamber has a test volume of about 500 L (80 cm × 80 cm × 80 cm) whereby relative humidity can be varied from about 95 % down to 2 % over a temperature range between 300 and 200 K and pressure range between 1000 and 100 hPa. Two reference instruments are connected to the chamber, an LPF hygrometer (Kley and Stone, 1978; Helten et al., 1998) which has an accuracy of ±3 % in the VMR range of 1–1000 ppmV, and a dew/frost point hygrometer (General Eastern, Type D1311R) which has an ±0.5 K uncertainty in the saturation temperature above 1000 ppmV.

During the measurements which were performed in the 2–12 000 ppmV VMR range at different pressures, the input lines for the two PA cells were joined by a tee connector. The air from the chamber was sampled through a 1.5 m length 1/8 inch heated stainless steel tube. Its inlet was placed as close as possible to the inlets of the reference instruments.

AMTD
7, 6359–6384, 2014

As the three instruments have different temporal resolutions, the results were interpolated to the time resolution of the PA system using cubic spline method. From the resulting datasets the relative deviation values, slopes of the cross plots and the Pearson correlation values were determined.

2.5 Airborne tests

WaSul-Hygro was tested in a four flight campaign dedicated to compare various systems measuring WV VMR within the DENCHAR (Development and Evaluation of Novel Compact Hygrometer for Airborne Research) project, which is part of the European Community's 7th Framework Program funded project EUFAR (European Facility for Airborne Research). The platform was a Learjet35A (Bombardier) research airplane operated by GFD GmbH (Hohn Germany). The PA system was compared to the FISH (Zöger et al., 1999) (Fast In-situ Stratospheric Hygrometer) instrument (measurement frequency of 1 Hz, a noise equivalent mixing ratio of 0.2–0.15 ppmV at 3 ppmV and a lower/upper detection limit of 0.18–0.13/1500 ppmV) and with a commercially available PICARRO G2401-m WS-CRDS system (Picarro Inc., Santa Clara, CA, USA) (Chen et al., 2010). During the campaign before and after each flight FISH was calibrated against a chilled mirror hygrometer (MBW DP30) with the help of a saturation-dilution based humidity generator. The WS-CRDS system measures simultaneously CO_2, CH_4, CO and H_2O and it is specifically designed for flight operation; it was operated at 186.6 hPa (140 Torr). Its measurement time is about 2.5 s; and by lowering its sample flow rate down to 0.1 slpm it was able to measure at altitude level up to 12.5 km without using a sample pump upstream of the sample cell. The instrument itself is not factory calibrated but another WS-CRDS instrument was calibrated against a chilled mirror hygrometer (Dewmet, Michell instruments Ltd., UK) at Max Planck Institute for Biogeochemistry, (Jena, Germany), and the calibration constants were transferred to all subsequently manufactured CRDS instruments by Picarro Inc (Crosson, 2008). During the campaign it was compared against the calibration stand used to calibrate FISH revealing an offset of 14.5 ppmV which was subtracted from the CRDS flight data.

AMTD
7, 6359–6384, 2014

Unfortunately due to logistic reasons the three instruments took their sample from three different inlets. The inlets of the PA cells were again joined together and were connected to a backward facing aircraft inlet in order to measure WV VMR by a heated stainless steel tube having outer diameter of 1/8″ and length of 1.5 m. FISH was connected to a forward facing inlet through a 0.5 m long, 10 mm inner diameter heated stainless steel tube to measure TW VMR, while the WS-CRDS system was connected to a forward facing de-iced Rosemount TAT housing (model 102BX) through a FEP-tube of 1 m length and 1.58 mm inner diameter to measure WV VMR. For the Wasul-Hygro the flow was provided by a pump, while the WS-CRDS and FISH systems used the ram-pressure provided by the samplers together with a downstream sampling pump.

Due to various reasons large portions of the measured data are not suitable for inter-comparison purposes as follows. The central data logging computer crashed repeatedly, causing data losses of five to ten minute periods. Considerable deviations between the readings of the three systems were observed during periods whenever the measured VMR varied rapidly, most probably due to the different response times of the sampling lines. WS-CRDS values below 50 ppmV had to be neglected as their reliability is under discussion. The performance of the FISH was acceptable only during the last two flights due to a small internal leak, which was discovered and fixed only after the second flight. From the FISH dataset all measured values above 350 ppmV had to be neglected. During occasional presence of clouds the FISH data had to be neglected as its TW VMR data differed from the WV VMR reading of the other two instruments.

The comparable parts of the measured data were evaluated as done in case of the ESF chamber comparison.

AMTD
7, 6359–6384, 2014

3 Results and discussion

3.1 Calibration

The calibration curves for the two WaSul-Hygro channels at one of the calibration pressures (200 hPa) together with the programmed SM switching points can be seen in Fig. 3. The measured sensitivities and noise levels (1σ) below 10 ppmV for the two measuring cells at 200 hPa pressure with 600-fold amplification of the microphone signal are 120 nV ppmV^{-1} and 54 nV and 118 nV ppmV^{-1} and 59 nV respectively. At higher VMRs similar sensitivities but larger noise levels (typically 0.5 % of the actual VMR reading) were found. Calibration curves at other pressures yield similar sensitivities and noise levels. From these results it follows that the repeatability of the WV VMR measurements is for either cell is 0.5 ppm or 0.5 % of the actual reading (whichever is greater). In Fig. 4 the sensitivity of the PA system as the function of pressure at different VMR-s is shown. The dependences are very similar for the two cells. It can be clearly seen that the use of the simplifying assumption of VMR independent sensitivities (as done previously, Szakáll et al., 2006) would lead to highly inaccurate VMR determination.

As the calibration curves are not completely linear, they have to be approximated with high (up to 10) order polynomials for both channels, for both SMs, at each pressure. These polynomials form the calibration surface as mentioned before (Sect. 2.2.4).

The VMR calculation method applied during laboratory tests shown traceability to the humidity generator within less than 0.5 % ± 0.5 ppmV at any VMR-s and at any pressures for both PA cells.

3.2 Laboratory inter-comparison

During the laboratory measurements at the ESF chamber the VMR values measured by the two channels of the PA system coincided within noise level or within 0.5 %. These results are practically identical to the observed ones during laboratory calibration. One

AMTD
7, 6359–6384, 2014

representative result of the laboratory inter-comparison at FZJ is shown in Fig. 5a, where also two SM switching points are indicated. In Fig. 5b the comparison cross plot between WaSul-Hygro and the reference instrument can be seen. The lower parts of Fig. 5a and b are the measured relative deviations as the function of time or VMR respectively with horizontal line indicated ±5 % limits.

Values measured in the fast cooling and drying periods when the ESF chamber is far from its steady state and values in case of fast VMR change when the chamber was not in its quasi steady state were omitted from the comparison. An example for these posteriorly omitted data in the range of 5–7000 ppmV can be seen in the deviation plot (Fig. 5b) where the loopy behavior indicates that the sampling line of the PA system could not follow the fast VMR variation in the chamber as fast as the reference instruments inside. It is important to note that the relative deviation in the presented case is still below 10 %. During the quasi steady state parts of the measurements the relative deviation (the difference between the VMR reading of the WaSul-Hygro and the reference instrument divided by the WaSul-Hygro reading) is less than 5 % or noise level in the 15–12 000 ppmV range. Other parameters of comparison can be found in the first line of Table 1.

3.3 Airborne tests

During the flight tests the noise level of the PA system and the deviation between the two sampling lines were roughly the same as during laboratory inter-comparison.

The comparisons of WaSul-Hygro, with FISH and WS-CRDS instruments can be seen in Figs. 6 and 7, respectively in a similar way as previously the results of the comparison at the ESF chamber but in case of the comparison with FISH ±25 % limits are shown. An SM switching point and a period when the measurement results of the two instruments deviate considerably (most probably due to differences of the sampling lines) are marked in Fig. 7a. The comparison results can be found in details in Table 1.

The slope of the cross plot between FISH and Wasul-Hygro deviates with about 20 % from the slope of the cross plot between Wasul-Hygro and the WS-CRDS system which

AMTD
7, 6359–6384, 2014

is close to the ideal 1. The facts that the cross plot in Fig. 6b is close to linear and the corresponding Pearson correlation coefficient is still high indicate that the deviation of FISH is most probably not due to a random effect or instrument malfunction such as noise. Furthermore the deviation cannot be related to occasional occurrence of cloud droplets or ice crystals in the gas stream sampled by the TW inlet of the FISH, because these events were carefully eliminated from the inter-comparison. Therefore it is rather a phenomenon which indicates that the WV VMR was indeed systematically different for the other sampling inlets and definitely requires further study.

3.4 Overall performance and outlook

Besides the performance parameters discussed above in details it is important to note that non-validated and therefore not presented tests show that the precision and accuracy values 18 months after the calibration did not vary significantly. These results still have to be verified and validated through more rigorous blind tests.

The actual size and weight of the system is acceptable on research aircrafts but to be mounted on an in-service one as standard these values still have to be improved. That is why a new controlling electronics is just being developed which besides the significant size reduction will be capable for real-time VMR calculation without the need of an external PC.

Acknowledgements. The authors would like to honor the memory of Cornelius Schiller (1961–2012), the former leader of the FISH development team and a worldwide recognized leading scientist of atmospheric humidity measurements.

The research leading to these results has received funding EUFAR contract no. 227159. The project has been partially funded by "TÁMOP-4.2.2.A-11/1/KONV-2012-0047" supported by the European Union and co-financed by the European Social Fund. The project has been also partially supported by the Hungarian Research and Technology Innovation Fund (OTKA), project number 109679. D. Tátrai was partially supported by "TÁMOP 4.2.4.A/2-11-1-2012-0001" supported by the European Union and Hungary and co-financed by the European Social Fund. For the operation of the Picarro WS-CRDS system funding from IAGOS-ERI (In-service Aircraft for

AMTD
7, 6359–6384, 2014

a Global Observing System – European Research Infrastructure, contract no. 212128), part of the EU's 7th Framework Programme, was used.

References

Bell, A. G.: On the production and reproduction of sound by light: the photophone, Am. J. Sci., 3, 305–324, 1880.

Bell, A. G.: The production of sound by radiant energy, Science, 2, 242–253, 1881.

Bozóki, Z., Pogány, A., and Szabó, G.: Photoacoustic instruments for practical applications: present, potentials, and future challenges, Appl. Spectrosc. Rev., 46, 1–37, doi:10.1080/05704928.2010.520178, 2011.

Bozóki, Z., Tátrai, D., and Szabó, G.: Method and arrangement for wavelength monitoring of wavelength tunable light source and stabilizing based on absorption spectroscopic detecting, Hungarian patent, HU1100719 (A2), 2013.

Brenninkmeijer, C. A. M., Crutzen, P., Boumard, F., Dauer, T., Dix, B., Ebinghaus, R., Filippi, D., Fischer, H., Franke, H., Frieß, U., Heintzenberg, J., Helleis, F., Hermann, M., Kock, H. H., Koeppel, C., Lelieveld, J., Leuenberger, M., Martinsson, B. G., Miemczyk, S., Moret, H. P., Nguyen, H. N., Nyfeler, P., Oram, D., O'Sullivan, D., Penkett, S., Platt, U., Pupek, M., Ramonet, M., Randa, B., Reichelt, M., Rhee, T. S., Rohwer, J., Rosenfeld, K., Scharffe, D., Schlager, H., Schumann, U., Slemr, F., Sprung, D., Stock, P., Thaler, R., Valentino, F., van Velthoven, P., Waibel, A., Wandel, A., Waschitschek, K., Wiedensohler, A., Xueref-Remy, I., Zahn, A., Zech, U., and Ziereis, H.: Civil Aircraft for the regular investigation of the atmosphere based on an instrumented container: The new CARIBIC system, Atmos. Chem. Phys., 7, 4953–4976, doi:10.5194/acp-7-4953-2007, 2007.

Buldyreva, J., Lavrentieva, N., and Starikov, V.: Collisional Line Broadening And Shifting Of Atmospheric Gases; a Practical Guide for Line Shape Modelling by Current Semi-Classical Approaches, Imperial College Press, London, UK, 2011.

CARIBIC: CARIBIC database, available at: http://www.caribic-atmospheric.com/ (last access: 11 April 2014), 2014.

Castleden, S. L., Kirkbright, G. E., and Spillane, D. E. M.: Wavelength modulation in photoacoustic spectroscopy, Anal. Chem., 53, 2228–2231, doi:10.1021/ac00237a019, 1981.

AMTD

7, 6359–6384, 2014

Chen, H., Winderlich, J., Gerbig, C., Hoefer, A., Rella, C. W., Crosson, E. R., Van Pelt, A. D., Steinbach, J., Kolle, O., Beck, V., Daube, B. C., Gottlieb, E. W., Chow, V. Y., Santoni, G. W., and Wofsy, S. C.: High-accuracy continuous airborne measurements of greenhouse gases (CO_2 and CH_4) using the cavity ring-down spectroscopy (CRDS) technique, Atmos. Meas. Tech., 3, 375–386, doi:10.5194/amt-3-375-2010, 2010.

Crosson, E. R.: A cavity ring-down analyzer for measuring atmospheric levels of methane, carbon dioxide, and water vapor, Appl. Phys. B, 92, 403–408, doi:10.1007/s00340-008-3135-y, 2008.

Goff, J. A. and Gratch, S.: Low-pressure properties of water from −160 to 212 °F, Trans. Amer. Soc. Heat. Vent. Eng., 52, 95–122, 1946.

Helten, M., Smit, H. G. J., Straeter, W., Kley, D., Nedelec, P., Zöger, M., and Busen, R.: Calibration and performance of automatic compact instrumentation for the measurement of relative humidity from passenger aircraft, J. Geophys. Res., 103, 643–652, doi:10.1175/2007JTECHA975.1, 1998.

IAGOS: available at: http://www.iagos.org/ (last access: 11 April 2014), 2014.

Kley, D. and Stone, E. J.: Measurement of water vapor in the stratosphere by photodissociation with Ly (a) (1216 A) light, Rev. Sci. Instrum., 49, 691–697, doi:10.1063/1.1135596, 1978.

Marenco, A., Thouret, V., Nédélec, P., Smit, H. G. J., Helten, M., Kley, D., Karcher, F., Simon, P., Law, K., Pyle, J., Poschmann, G., Wrede, R. V., Hume, C., and Cook, T.: Measurement of ozone and water vapor by Airbus in-service aircraft: the MOZAIC airborne program, an overview, J. Geophys. Res.-Atmos., 103, 25631–25642, doi:10.5194/acp-6-1053-2006, 1998.

McDonald, F. A. and Wetsel Jr., G. C.: Generalized theory of the photoacoustic effect, J. Appl. Phys., 49, 2313–2322, doi:10.1063/1.325116, 1978.

Miklós, A., Hess, P., and Bozóki, Z.: Application of acoustic resonators in photoacoustic trace gas analysis and meteorology, Rev. Sci. Instrum., 72, 1937–1955, doi:10.1063/1.1353198, 2001.

Saarela, J., Toivonen, J., Manninen, A., Sorvajärvi, T., and Hernberg, R.: Wavelength modulation waveforms in laser photoacoustic spectroscopy, Appl. Optics, 1, 743–748, doi:10.1364/AO.48.000743, 2009.

Schilt, S. and Thevenaz, L.: Wavelength modulation photoacoustic spectroscopy: theoretical description and experimental results, Infrared Phys. Techn., 48, 154–162, doi:10.1016/j.infrared.2005.09.001, 2006.

AMTD
7, 6359–6384, 2014

Seufert, J., Fischer, M., Koeth, J., Werner, R., Kamp, M., and Forchel, A.: DFB laser diodes in the wavelength range from 760 nm to 2.5 µm, Spectrochim. Acta A, 60, 3243–3247, doi:10.1016/j.saa.2003.11.043, 2004.

Sharpe, S. W., Johnson, T. J., Sams, R. L., Chu, P. M., Rhoderick, G. C., and Johnson, P. A.: Gas-phase databases for quantitative infrared spectroscopy, Appl. Spectrosc., 58 1452–1461, 2004.

Smit, H. G. J., Strater, W., Helten, M., and Kley, D.: Environmental simulation facility to calibrate airborne ozone and humidity sensors, Tech. Rep. Juel. Berichte Nr. 3796, Forschungszentrum Jülich, available at: http://www.fz-juelich.de/SharedDocs/Downloads/IEK/IEK-8/EN/ESF/ESF.pdf (last access: 11 April 2014), 2000.

Solomon, S., Qin, D., Manning, M., Chen, Z., Marquis, M., Averyt, K. B., Tignor, M., and Miller, H. L.: Climate Change 2007: The Physical Science Basis, Contribution of Working Group I to the Fourth Assessment Report of the Intergovernmental Panel on Climate Change, Cambridge University Press, Cambridge, UK and New York, NY, USA, 2007.

Szakáll, M., Huszár, H., Bozóki, Z., and Szabó, G.: On the pressure dependent sensitivity of a photoacoustic water vapor detector using active laser modulation control, Infrared Phys. Techn., 48, 192–201, doi:10.1016/j.infrared.2006.01.002, 2006.

Szakáll, M., Csikós, J., Bozóki, Z., and Szabó, G.: On the temperature dependent characteristics of a photoacoustic water vapor detector for airborne application, Infrared Phys. Techn., 51, 113–121, doi:10.1016/j.infrared.2007.04.001, 2007.

Tátrai, D., Bozóki, Z., and Szabó, G.: Method for wavelength locking of tunable diode lasers based on photoacoustic spectroscopy, Opt. Eng., 52, 096104, doi:10.1117/1.OE.52.9.096104, 2013.

WMO: Report No. 8, Guide to meteorological instruments and methods of observation, measurement of atmospheric humidity, 5th edn., World Meteorological Organization, Geneva, 1983.

Woodward, S. L., Parayanthal, P., and Koren, U.: The effects of aging on the Bragg section of a DBR laser, Photonics Technology Letters, 5, 750–752, doi:10.1109/68.229794, 1993.

Zöger, M., Afchine, A., Eicke, N., Gerhards, M. T., Klein, E., McKenna, D. S., Mörschel, U., Schmidt, U., Tan, V., Tuitjer, F., Woyke, T., and Schiller, C.: Fast in situ stratospheric hygrometers: a new family of balloonborne and airborne Lyman-α photofragment fluorescence hygrometers, J. Geophys. Res., 104, 1807–1816, doi:10.1029/1998JD100025, 1999.

AMTD
7, 6359–6384, 2014

Table 1. Results from comparisons of WaSul-Hygro with other instruments during laboratory and flight tests. In case of the comparison with the WS-CRDS system above 4000 ppmV there were no comparable amount of data available so the upper limits of the 2 and 5 % coincidence are certainly higher.

Reference instrument	Relative difference ranges from reference instruments (ppmV)			Pearson correlation	Slope of cross plot
	within noise level	2 %	5 %	coefficient	line
ESF chamber	< 150	200–750	15–12 000	0.99948	1.015
WS-CRDS	< 300	1500–4000	100–4000	0.99986	1.047
FISH	< 20	NA	NA	0.9965	0.86

AMTD
7, 6359–6384, 2014

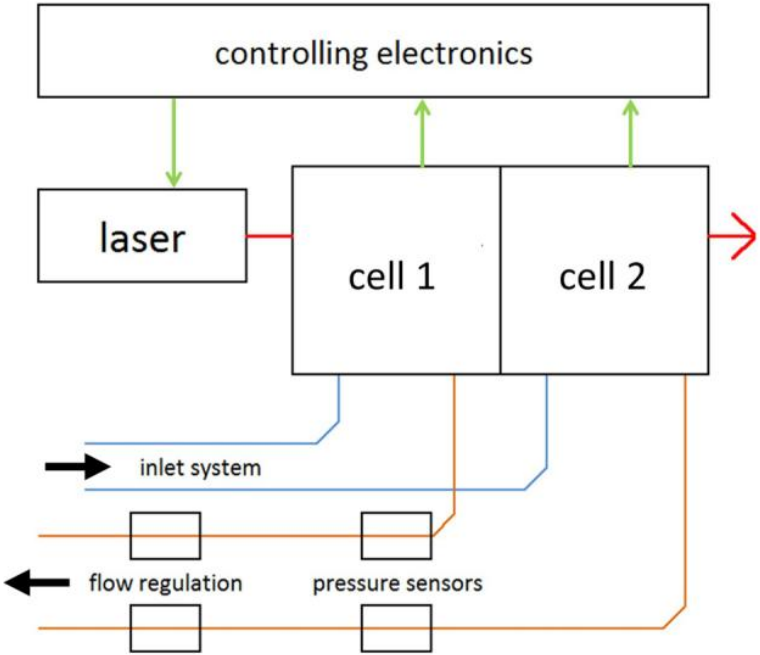

Figure 1. Schematic layout of the photoacoustic system. Green, red and black arrows indicate the electronic communication, laser beam propagation and gas flow directions, respectively. Blue and orange lines represent heated gas input and unheated gas output tubes, respectively.

AMTD
7, 6359–6384, 2014

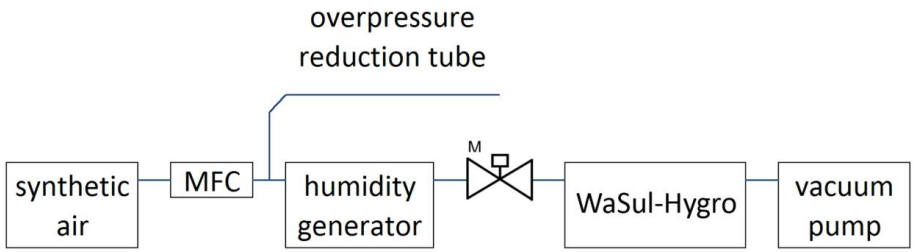

Figure 2. The schematic layout of the calibration system. MFC stands for mass flow controller and M is the stepper motor controlled needle valve (see text for details).

AMTD
7, 6359–6384, 2014

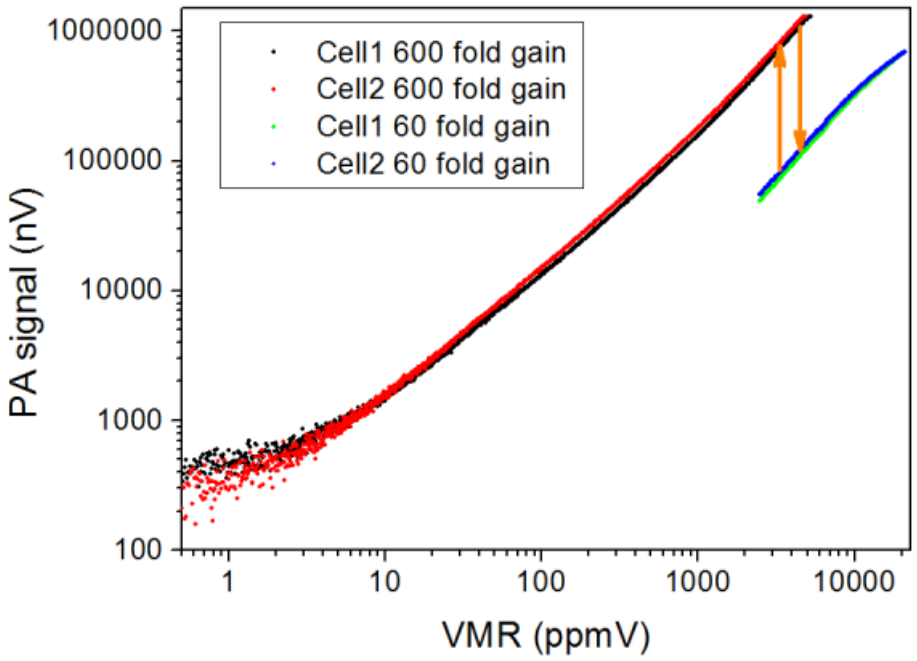

Figure 3. Calibration results at the pressure of 200 hPa. Arrows represent the SM switching points.

AMTD
7, 6359–6384, 2014

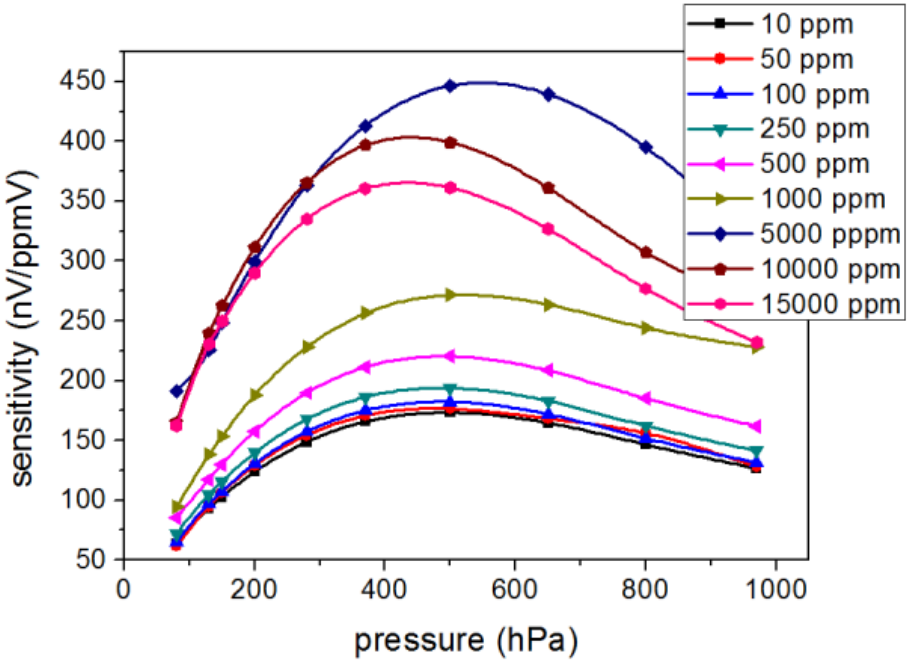

Figure 4. Dependence of the sensitivity of the PA system as the function of pressure at various VMRs.

AMTD
7, 6359–6384, 2014

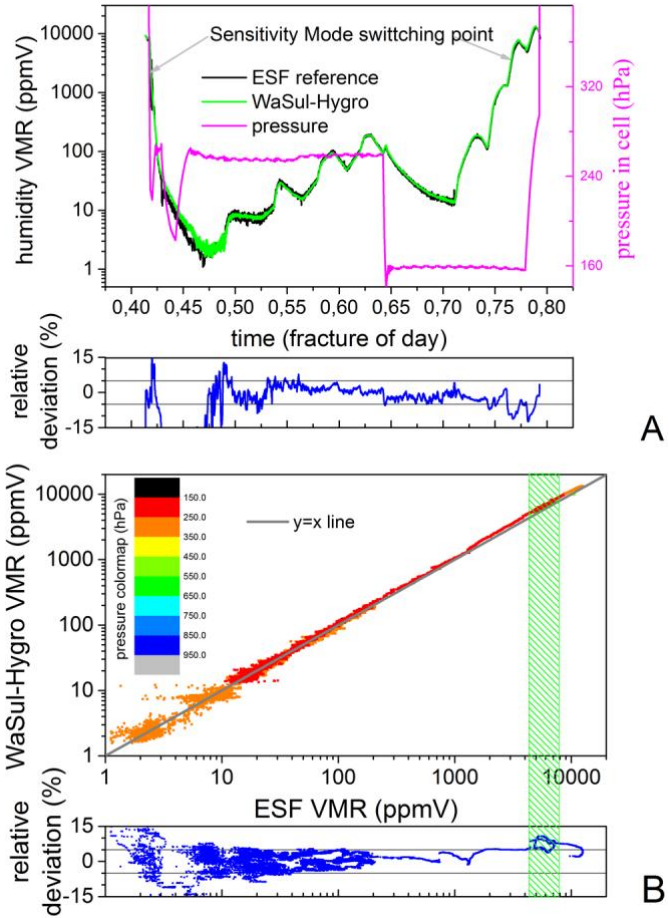

Figure 5. A representative measurement at the ESF chamber (5 May 2011). **(A)** is the time series of the measurements; **(B)** is the corresponding cross plot, where the pressure is coded by color and the green shaded area indicates the omitted loopy part.

AMTD
7, 6359–6384, 2014

Dual channel photoacoustic hygrometer for airborne measurements

D. Tátrai et al.

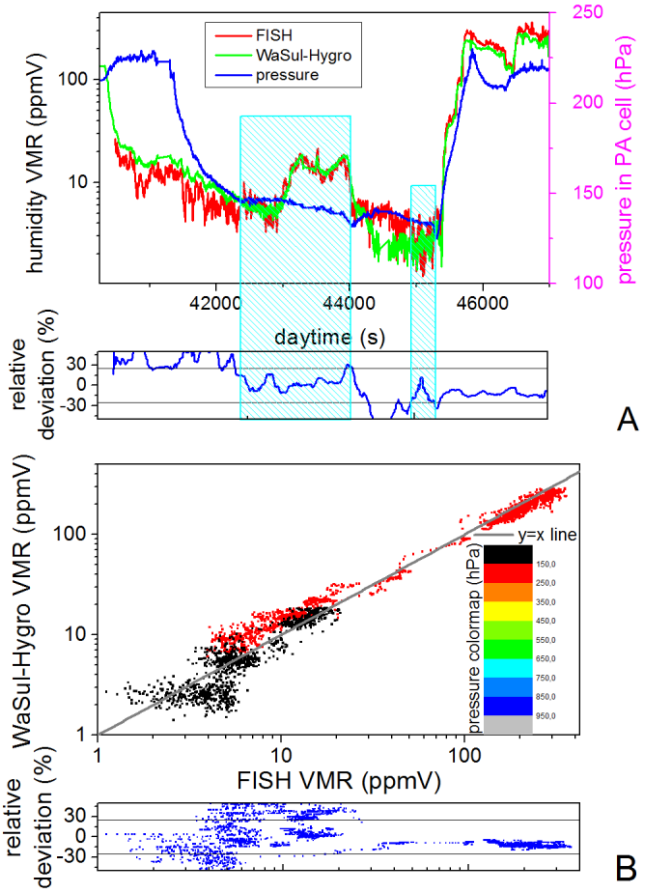

Figure 6. A representative comparison of WaSul-Hygro and FISH (DENCHAR flight 31 May 2011). **(A)** is the time series of the measurements where the blue shaded areas indicate when the two systems were measuring the same values within noise level; **(B)** is the corresponding cross plot, where the pressure is coded by color.

AMTD
7, 6359–6384, 2014

Dual channel photoacoustic hygrometer for airborne measurements

D. Tátrai et al.

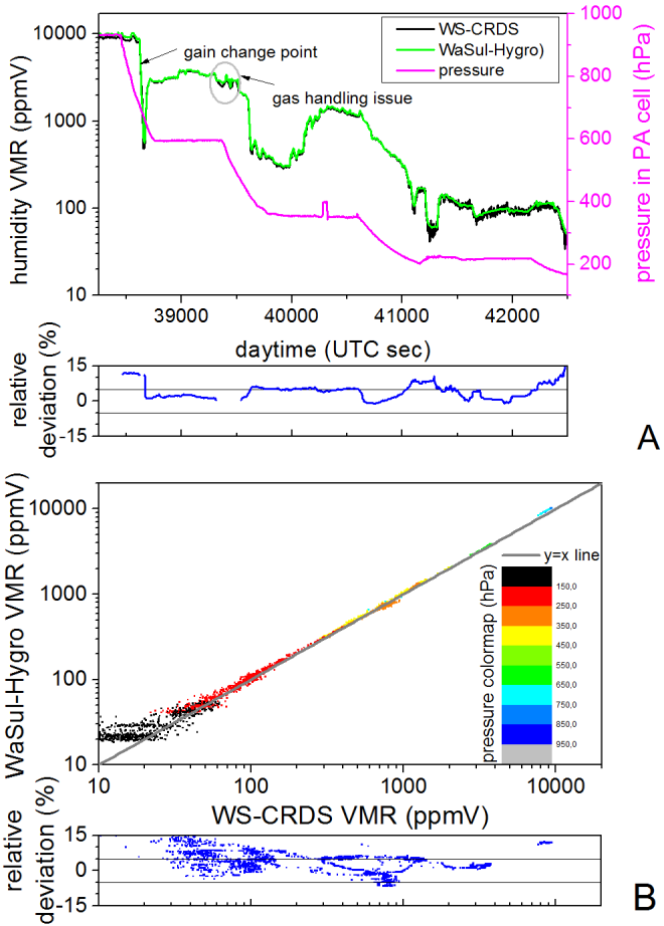

Figure 7. A representative comparison flight measurement of WaSul-Hygro and the WS-CRDS system (DENCHAR flight 26 May 2011). **(A)** is the time series of the measurements; **(B)** is the corresponding cross plot, where the pressure is coded by color.

AMTD
7, 6359–6384, 2014

Dual channel photoacoustic hygrometer for airborne measurements

D. Tátrai et al.